RESEARCH ARTICLE

Key Points:
- Suspended, slow-, and fast-sinking particulate organic carbon (POC) contributes 94:6:<1% to total POC concentration, respectively
- POC flux below the mixed layer is often dominated by slow-sinking particles
- In situ generation of slow-sinking POC below the mixed layer, via midwater fragmentation, may lead to shallower mineralization of particles

Slow-sinking particulate organic carbon in the Atlantic Ocean: Magnitude, flux, and potential controls

Chelsey A. Baker[1,2], Stephanie A. Henson[1], Emma L. Cavan[1,2,3], Sarah L. C. Giering[1], Andrew Yool[1], Marion Gehlen[4], Anna Belcher[1,2], Jennifer S. Riley[1], Helen E. K. Smith[1], and Richard Sanders[1]

[1]National Oceanography Centre, Southampton, UK, [2]Ocean and Earth Science, University of Southampton, National Oceanography Centre, Southampton, UK, [3]Now at Institute for Marine and Antarctic Studies, University of Tasmania, Hobart, Tasmania, Australia, [4]LSCE/IPSL, Laboratoire des Sciences du Climat et de l'Environnement, CEA-CNRS-UVSQ Orme des Merisiers, Gif-sur-Yvette, France

Abstract The remineralization depth of particulate organic carbon (POC) fluxes exported from the surface ocean exerts a major control over atmospheric CO_2 levels. According to a long-held paradigm most of the POC exported to depth is associated with large particles. However, recent lines of evidence suggest that slow-sinking POC (SS_{POC}) may be an important contributor to this flux. Here we assess the circumstances under which this occurs. Our study uses samples collected using the Marine Snow Catcher throughout the Atlantic Ocean, from high latitudes to midlatitudes. We find median SS_{POC} concentrations of 5.5 µg L^{-1}, 13 times smaller than suspended POC concentrations and 75 times higher than median fast-sinking POC (FS_{POC}) concentrations (0.07 µg L^{-1}). Export fluxes of SS_{POC} generally exceed FS_{POC} flux, with the exception being during a spring bloom sampled in the Southern Ocean. In the Southern Ocean SS_{POC} fluxes often increase with depth relative to FS_{POC} flux, likely due to midwater fragmentation of FS_{POC}, a process which may contribute to shallow mineralization of POC and hence to reduced carbon storage. Biogeochemical models do not generally reproduce this behavior, meaning that they likely overestimate long-term ocean carbon storage.

1. Introduction

The biological carbon pump exerts a major control over atmospheric CO_2 levels, transferring carbon from the surface ocean to the deep [*Volk and Hoffert*, 1985; *Kwon et al.*, 2009], mainly via the gravitational sinking of particulate organic carbon (POC). The fraction of POC leaving the upper ocean that reaches the deep ocean is controlled by particle sinking speed, and the rate particles are respired, which together define the remineralization depth [*Boyd and Trull*, 2007; *Kwon et al.*, 2009].

Detrital POC in the ocean can be divided into three pools, loosely defined as follows: fast sinking (FS_{POC}; > 20 m d^{-1}), slow sinking (SS_{POC}; < 20 m d^{-1}), and suspended [*Riley et al.*, 2012]. The current paradigm is that fast-sinking particles dominate flux to the seafloor [*Billett et al.*, 1983], as slow-sinking particles are likely remineralized at shallower depths [*Suess*, 1980; *Buesseler et al.*, 2007]. If climate change induces a shift in phytoplankton community from diatoms to nanophytoplankton, in response to increasing stratification, the average depth of remineralization is likely to reduce [*Bopp et al.*, 2005] and the potential for future ocean carbon storage may also decrease [*Alldredge and Silver*, 1988; *Kwon et al.*, 2009].

Slow-sinking particles are typically assumed to be small though large particles with low excess densities may also sink slowly [*Durkin et al.*, 2015]. SS_{POC} is generally thought to originate from small plankton (nanoplankton or picoplankton), which could dominate in the euphotic zone of oligotrophic and postbloom regions [*Stewart et al.*, 2010]. SS_{POC} may penetrate beyond the upper mesopelagic if remineralization rates are slow (i.e., cold environments) [*Iversen and Ploug*, 2013] or may be transported to depth via the mixed layer pump, through turbulent mixing of small particles that become trapped below the thermocline by a shoaling mixed layer [*Gardner et al.*, 1995; *Dall'Olmo and Mork*, 2014]. Other studies suggest that SS_{POC} originates from the physical disaggregation [*Burd and Jackson*, 2009; *Close et al.*, 2013], physical fragmentation via turbulence [*Stemmann et al.*, 2004], or biological fragmentation of large particles [*Giering et al.*, 2014; *Mayor et al.*, 2014]. Proposed mechanisms of biotic fragmentation include direct fragmentation due to swimming organisms [*Dilling and Alldredge*, 2000], zooplankton capturing and rejecting fecal pellets (FPs) [*Lampitt et al.*, 1990;

Iversen and Poulsen, 2007], zooplankton sloppy feeding [*Jumars et al.*, 1989; *Giering et al.*, 2014], and microbial gardening, in which zooplankton fragment organic particles stimulating the growth of nutritious protists [*Mayor et al.*, 2014].

Recent work suggests that slow-sinking particles may make a significant contribution to POC flux (up to 60% of total observed flux at <260 m), between summer and early winter with a small contribution (~ 10%) between winter and summer [*Peterson et al.*, 2005; *Alonso-González et al.*, 2010]. Particle sinking speeds calculated using ^{210}Po-^{210}Pb profiles found slow-sinking particles (< 100 m d^{-1}) to be the main contributor to flux in the North Atlantic, except in temperate regions during a bloom [*Villa-Alfageme et al.*, 2016]. This method also estimated that average sinking speed increased with depth, suggesting remineralization of slow-sinking particles in the upper mesopelagic [*Villa-Alfageme et al.*, 2014]. Small particles have been estimated to contribute 18–78% of total POC flux at 125–500 m depth in the surface ocean [*Durkin et al.*, 2015], suggesting that observations which overlook small particles may underestimate the flux of POC out of the upper mesopelagic.

Slow-sinking particles are systematically undercollected by upper ocean sediment traps [*Buesseler et al.*, 2007]. In addition, in situ SS$_{POC}$ sampling methods typically use average sinking speeds or size-based assumptions, which are often poorly constrained, to calculate flux [*Riley et al.*, 2012; *Durkin et al.*, 2015], which may lead to inaccuracies in the contribution of slow-sinking fluxes. Underestimation of the SS$_{POC}$ pool may partially explain the discrepancy between the respiration demand and supply in the lower mesopelagic zone [*Giering et al.*, 2014]. Much of our knowledge about the formation, export, and flux of SS$_{POC}$ is based on theory, experiments, indirect measurements, or models [*Villa-Alfageme et al.*, 2014; *Durkin et al.*, 2015] rather than direct observation [*Riley et al.*, 2012]. However, the use of indented rotating-sphere sediment traps allows for POC and sinking speed of particles to be measured simultaneously [*Peterson et al.*, 2005; *Alonso-González et al.*, 2010].

A key question is whether SS$_{POC}$ found in the upper mesopelagic is exported from the photic zone or is generated in situ via the fragmentation of larger particles. *Riley et al.* [2012] hypothesized that SS$_{POC}$ represents the constant background POC flux from the euphotic zone which is remineralized in the upper mesopelagic, while FS$_{POC}$ flux occurs as a result of processes such as the spring bloom and sinks to the deep ocean. [*Riley et al.*, 2012]. Amino acid and pigment biomarkers suggest that SS$_{POC}$ can have the same degradation state, or be less degraded, than FS$_{POC}$ particles which were found to be heavily altered by microzooplankton and zooplankton grazing [*Lee et al.*, 2000; *Alonso-González et al.*, 2010]. When considering the rapid turnover rate of slow-sinking particles [*Goutx et al.*, 2007; *Cavan et al.*, 2017a], and the similar degradation states, this implies that SS$_{POC}$ in the upper mesopelagic must be generated in situ, possibly from fragmentation of larger, fast-sinking particles [*Mayor et al.*, 2014; *Giering et al.*, 2014; *Belcher et al.*, 2016a; *Cavan et al.*, 2017b].

Biogeochemical models often contain multiple classes of particles segregated by sinking speed; however, the relative contributions these classes make to modeled flux or the importance of various processes to particle production has rarely been reported. However, a recent model study found that slow-sinking particles contributed up to 100% of export in the subtropical gyres and Arctic Ocean, which has yet to be observed in situ [*Henson et al.*, 2015].

A greater understanding of SS$_{POC}$, in terms of its origin, processing in the upper water column and residence time is needed to evaluate the role of SS$_{POC}$ in carbon budgets and their accurate representation in biogeochemical models. In this study we compile estimates of the magnitude of the fast-sinking, slow-sinking, and suspended POC pools and their contributions to POC flux from Marine Snow Catcher (MSC) data collected during eight middle- to high-latitude Atlantic Ocean cruises. These data provide information on the spatial variability in the magnitude of the POC pools, with a particular focus on the SS$_{POC}$ concentration and flux. We also utilize the NEMO-MEDUSA [*Yool et al.*, 2013] and PISCES [*Gehlen et al.*, 2006] biogeochemical models to further investigate the origins and controls on SS$_{POC}$ below the mixed layer depth (MLD), using the Atlantic sector of the Southern Ocean as a case study.

2. Methods

POC samples were collected using the MSC at 144 stations on eight cruises in the Atlantic Ocean, including the Atlantic sector of the Southern Ocean, between 2009 and 2013 (Figure 1; see also Data Set S1 in the
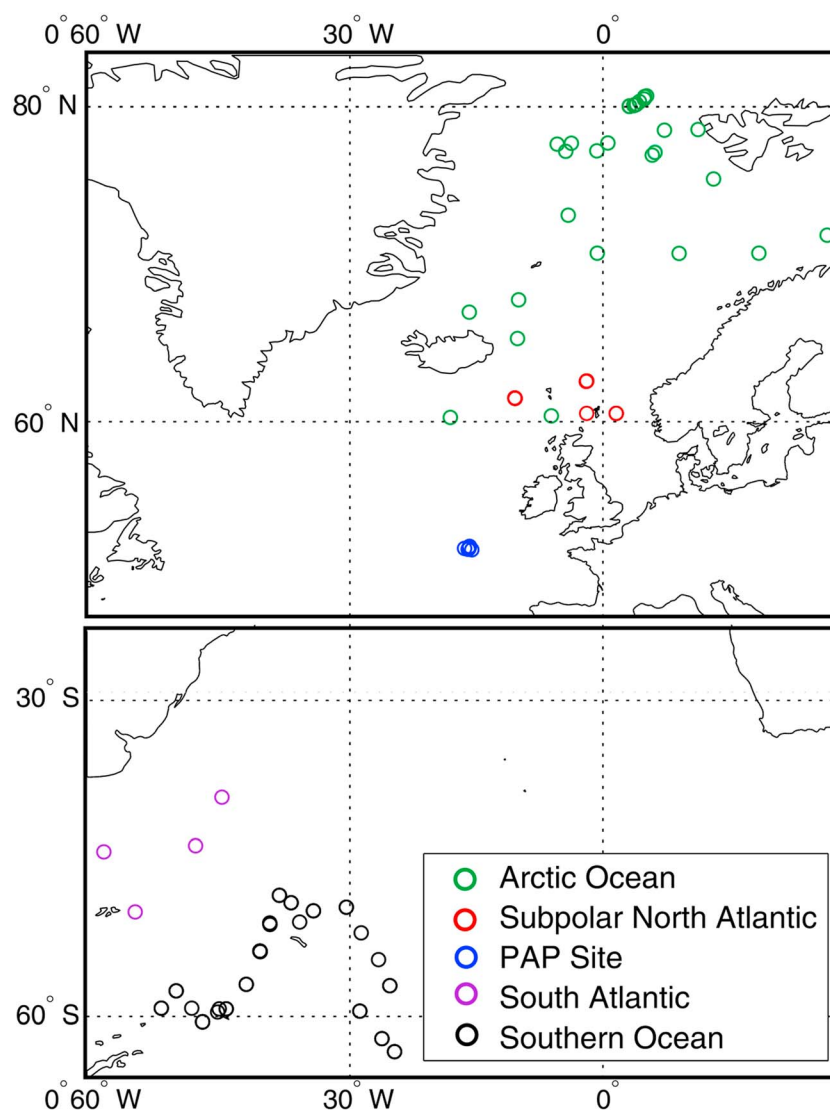
Figure 1. Sampling Stations in the Atlantic Ocean. Slow-sinking particulate organic carbon samples were collected using Marine Snow Catchers in the Arctic Ocean (JR219 and JR271; green), Subpolar North Atlantic (M87/1–2; red), North East Atlantic (PAP Site) (D341 and JC087; blue), South Atlantic Ocean (MV1101; purple) and the Southern Ocean (JR274 and JR291; black). In total 144 samples were collected (Data Set S1).

supporting information). Samples were collected during spring and summer. Each cruise was characterized in relation to the bloom state using satellite chlorophyll *a* (chl) data (Table 1 and Figure S1).

2.1. Marine Snow Catcher Principles

The MSC allows the measurement of the in situ fast-sinking, slow-sinking, and suspended POC pools. Specifics of the MSC deployment and methodology were first described in *Riley et al.* [2012] and have been expanded upon in *Giering et al.* [2016]. The MSC is a 95 L water sampler which is open when deployed, similar to a Niskin bottle. The MSC is fired at a specified depth below the MLD and left to settle on deck for 2 h. FS_{POC} particles ($> 100\ \mu m$) settle into a tray in the MSC base. Particles reaching the 8 L base in the settling period are defined as SS_{POC} and particles remaining in the upper 87 L of the MSC defined as suspended POC.

MSCs were deployed using one of two deployment strategies: either one sample was taken below the mixed layer in the upper 600 m of the water column, or two samples were taken in quick succession at MLD + 10 m and MLD + 110 m, to estimate remineralization length scale in the upper mesopelagic zone. The first approach was employed on cruises to the PAP site [*Riley et al.*, 2012] and the Subpolar North Atlantic

Table 1. Median Slow-Sinking POC Flux (IQR) in mg m^{-2} d^{-1} and as a Percentage of Total POC Flux for Both the Giering and SETCOL Methods for Seven Atlantic Ocean Cruises[a]

Region	Bloom State	Susp:Slow:Fast Average Concentration (%)	Slow-Sinking POC Flux			
			Giering (mg m^{-2} d^{-1})	Giering (% of Total Flux)	SETCOL (mg m^{-2} d^{-1})	SETCOL (% of Total Flux)
Arctic Ocean 2010	Secondary bloom	95.3: 4.6: 0.02	57.7 (27.8–107.4)	78.4 (40.6–98.9)	-	-
Arctic Ocean 2012	Spring bloom	91.8: 8.2: 0.002	629.0 (457.4–1184.1)	98.1 (96.7–99.0)	-	-
Subpolar North Atlantic 2012	Prebloom	90.3: 9.7: 0.002	89.6 (55.5–121.0)	97.0 (90.0–98.7)	96.6 (66.5–141.4)	93.5 (78.9–97.5)
PAP Site 2009	Post(small) bloom	94.9: 5.1: 0.03	114.2 (110.2–125.4)	76.5 (71.3–84.7)	-	-
PAP Site 2013	Prebloom	96.9: 2.7: 0.42	76.1 (35.6–108.1)	62.9 (48.3–76.8)	56.8 (39.5–72.1)	71.2 (67.1–71.6)
Southern Ocean 2013a	Post(/declining) bloom	94.3: 5.7: 0.001	120.6 (71.5–158.8)	91.7 (84.2–97.1)	145.0 (82.4–249.3)	94.5 (88.3–98.4)
Southern Ocean 2013b	Spring bloom	90.5: 9.4: 0.15	51.4 (34.0–119.2)	49.1 (46.3–71.6)	84.0 (30.0–160.0)	50.1 (43.5–73.6)

[a]The general bloom state is established from satellite chlorophyll a time series (Figure S1). Dashes represent cruises where it was not possible to calculate slow-sinking flux using the SETCOL method. The South Atlantic cruise is not included as only a few samples were collected.

[*Giering et al.*, 2016] and Arctic and South Atlantic cruises, and the second approach was employed consistently on the Southern Ocean cruises considered in section 3.4 [*Cavan et al.*, 2015; *Belcher et al.*, 2016a].

2.2. POC Concentration Calculations

POC concentrations of the three pools were calculated using the method described in *Riley et al.* [2012]. The fast-sinking particles were analyzed using a microscope camera, and the equivalent spherical diameter of each particle was calculated either using image processing software, such as Image J and SigmaScan Pro 4, or by measuring the diameter from photographs [*Riley et al.*, 2012; *Cavan et al.*, 2015; *Belcher et al.*, 2016a; *Giering et al.*, 2016]. The volume (mm^3) of each particle was then calculated following *Alldredge* [1998] and the carbon content estimated using the "all types" conversion factor (AL CF) in *Alldredge* [1998] for aggregates. For some cruises (see Data Set S1) a more detailed analysis of the particles was undertaken, classifying particles into phytodetrital aggregates and fecal pellets. The carbon content of fecal pellets was determined using the "fecal" conversion factor in *Alldredge* [1998]. Southern Ocean fast FS$_{POC}$ fluxes were additionally calculated using AL CF for phytodetrital aggregates and a conversion factor for fecal pellets (Alldredge + Manno CF: Al + MN CF) of 0.039 mg C mm^3 obtained from direct measurements of FP collected in sediment traps in the Southern Ocean [*Manno et al.*, 2015; *Cavan et al.*, 2017a]. We compare FS$_{POC}$ fluxes calculated via these two methods to assess whether our results are sensitive to the choice of CF. FS$_{POC}$ concentration was determined by summing the POC of all fast-sinking particles per MSC (POC$_{fast}$) and dividing by the volume of the MSC (V_{MSC}; equation (1)). Fast-sinking POC mass measurements have been assigned an uncertainty of 10% to account for errors in estimating the volume of the particles.

$$\text{FS}_{POC} \text{ Concentration } \left(\mu g \, L^{-1}\right) = \text{POC}_{fast}/V_{MSC} \qquad (1)$$

SS$_{POC}$ concentration was calculated by subtracting the POC concentration of the top section (suspended POC) from the POC concentration of the base of the MSC. The resulting concentration is multiplied by the ratio of the volume of the base to the top (8/95 L) to calculate the presettling (in situ) SS$_{POC}$ concentration (equation (2)) [*Riley et al.*, 2012]. Slow and suspended POC mass measurements have been assigned an uncertainty of 5%. All errors have been propagated using standard deviation and basic error propagation equations for addition/subtraction and multiplication/division and is reported as combined standard uncertainty (C.S.U), with all C.S.Us reported in Data Set S1.

$$\text{SS}_{POC} \text{ Concentration } \left(\mu g \, L^{-1}\right) = \left(c_{Base} - c_{Top}\right) \times 8/95 \qquad (2)$$

Median concentrations (with interquartile ranges, IQR) are reported for the Atlantic Ocean, to provide a generalized view of the fast, slow, and suspended concentrations and for each cruise for fast, slow, and suspended concentrations and fluxes, respectively.

2.3. POC Flux Calculations

POC fluxes were calculated from the mass of fast- or slow-sinking POC in the MSC (m_{fast} or m_{slow} in milligram) via the following equations [*Cavan et al.*, 2015; *Giering et al.*, 2016]. Daily fluxes were calculated to allow for comparison with other studies.

$$\text{Fast-Sinking Flux } \left(\text{mg m}^{-2}\text{ d}^{-1}\right) = \frac{m_{fast}}{A_{msc}} \times \frac{w_{fast}}{h} \tag{3}$$

$$\text{Slow-Sinking Flux Giering } \left(\text{mg d}^{-1}\right) = \frac{m_{slow}}{A_{msc}} \times \frac{w_{slow}}{h} \tag{4}$$

$$\text{Slow-Sinking Flux SETCOL } \left(\text{mg m}^{-2}\text{ d}^{-1}\right) = \frac{\left(m_{slow} + m_{susp}\right)}{A_{msc}} \times \frac{w_{bulk}}{h} \tag{5}$$

Here A_{msc} is the area of the base (0.058 m^2), h the height of the MSC (1.5 m), and w the sinking speed (in m d^{-1}). For fast-sinking particles the sinking speed was estimated on board using a measuring cylinder and the time taken for individual particles to sink a set distance [*Ploug et al.*, 2010; *Riley et al.*, 2012; *Belcher et al.*, 2016a], except for the cruise to the Northeast Atlantic in 2013, where a sinking rate was calculated using a flow chamber as in *Ploug and Jorgensen* [1999] (equation (3)). Uncertainty estimates were propagated and C.S.U reported with further specifics detailed in Data Set S1. These approaches cannot be used for slow-sinking material as particles are invisible to the naked eye. Two approaches have therefore been used to assess its contribution (equations (4) and (5)).

The *Giering et al.* [2016] approach is a development of the *Riley et al.* [2012] method. As FS_{POC} is picked using a pipette and a size specification (> 100 μm), the flux of the small POC (< 100 μm) that remains is defined by the dimensions of the MSC and the settling time. This method, based on the 2 h settling time and height of the MSC (equation (4)), implies an estimated mean sinking rate of ~18 m d^{-1} for the small sinking particles at all stations.

Becquevort and Smith [2001] used the SETCOL method, developed by *Bienfang* [1981], to calculate sinking rate. This method is similar to the Giering method, but rather than focussing on the small sinking particles only, SETCOL calculates the sinking rate of the initial "bulk" population of particles (all particles in the MSC excluding FS_{POC}, i.e., slow + suspended POC) and applies this to the bulk mass (equation (5)). Based on the change in POC in the top section during the settling time, equation (6) uses mean initial homogenous concentration of the top section (T_0) converted to mass and subtracted from the mass in the base. This is divided by the change in suspended POC mass in the MSC multiplied by the height of the MSC divided by the settling time (t). The suspended POC fraction is assumed to be nonsinking (i.e., sinking rate is 0 m d^{-1}), and hence, the SETCOL method results in a small median for the initial population for our data set, w_{bulk} = 1.0 (IQR 0.6–1.7) m d^{-1} but a median slow-sinking rate of 22.2 (IQR 14.2–29.4) m d^{-1}, similar to the Giering method.

T_0 was only sampled on the Southern Ocean cruises, in the Subpolar North Atlantic in 2012 and in the Northeast Atlantic (PAP Site) in 2013; therefore, the SETCOL SS_{POC} flux could only be calculated for these regions.

$$w_{bulk} \left(\text{m d}^{-1}\right) = \left(\left(\left(V_{base} \times C_{base}\right) - \left(V_{base} \times T_0\right)\right) / \left(V_{msc} \times T_0\right)\right) \times (h/t) \tag{6}$$

The median SS_{POC} flux is reported, along with the interquartile range for each cruise, to determine differences in magnitude spatially and temporally. The relative contributions of FS_{POC} and SS_{POC} to total flux were calculated to allow spatial and temporal comparisons (equation (7)).

$$\text{Relative } SS_{POC} \text{ Flux (\%)} = \left(SS_{POC} \text{ Flux} / \left(SS_{POC} \text{ Flux} + FS_{POC} \text{ Flux}\right)\right) \times 100 \tag{7}$$

Additionally, to quantify changes in SS_{POC} flux, compared to the FS_{POC} flux, with depth in the Southern Ocean, the shallow (MLD + 10 m) SS_{POC} flux relative contribution (%) was subtracted from the deep (MLD + 110 m) SS_{POC} flux relative contribution (%).

2.4. Attenuation Parameters

The microbial respiration rate of FS_{POC} and SS_{POC} fluxes were calculated for the Southern Ocean cruises using the rates measured in *Cavan et al.* [2017b] to estimate the depth to which each exported POC fraction can penetrate. The respiration rates were reported for 15°C so a temperature correction was applied using the Q10 equation (equation (8)) [*Yvon-Durocher et al.*, 2012] and the median temperature recorded during sampling for each cruise (2.61°C for the Southern Ocean 2013a (SO13a) and 0.66°C for the Southern Ocean 2013b (SO13b)). The respiration rate (k_1) measured at temperature (T_1) is used in the Q10 equation which denotes that every 10°C increase in temperature will lead to a k_1 rate 2.5 times greater. T_2 is the measured temperature were the unknown respiration rate (k_2) is being calculated. The mean respiration rates reported by *Cavan et al.* [2017b] were 0.13 d^{-1} for FS_{POC} and 5 d^{-1} SS_{POC}.

$$Q10 = \left(\frac{k_2}{k_1}\right)^{(10/(T_2-T_1))} \tag{8}$$

The microbial remineralization length scale (RLS) [*Boyd and Trull*, 2007], defined as the depth by which 63% of POC flux has been remineralized, was calculated using the median sinking rate divided by the calculated respiration rate for the FS_{POC} and SS_{POC} [*Cavan et al.*, 2017b].

2.5. Model Output

We investigated how successfully two biogeochemical models represented SS_{POC} flux. The NEMO-MEDUSA biogeochemical model has two pools of detrital material [*Yool et al.*, 2013]. The fast-sinking detrital fraction originates from diatom and mesozooplankton losses and is assumed to sink faster than the time step of the model can resolve, so is instantaneously remineralized at each vertical depth, with the attenuation of the flux profile determined by a ballast model [*Armstrong et al.*, 2002]. The slow fraction originates from nondiatom and microzooplankton losses, sinks at 3 m d^{-1}, and remineralizes at a temperature-dependant rate that is representative of microbial respiration [*Yool et al.*, 2013]. Unlike slow-sinking detritus, fast-sinking detritus is not grazed by zooplankton and there is no route to transfer material between the fast- and slow-sinking detrital pools. The model was run at 1/4° spatial resolution under model-derived interannually varying surface forcing with output available at 5 day resolution [*Yool et al.*, 2015]. The FS_{POC} and SS_{POC} fluxes (%) were extracted from the model at all the Southern Ocean sampling stations (locations detailed in Data Set S1) and averaged (12 years of output, 1995–2006) to create a climatological annual cycle, from which the fractional contribution of SS_{POC} flux was calculated (equation (7)) to allow for direct comparison to the observational data.

In the PISCES model, the detrital pool has big and small POC fractions with sinking rates of 50–200 m d^{-1} for large POC, which linearly increases with depth, and 3 m d^{-1} for small POC [*Aumont and Bopp*, 2006; *Gehlen et al.*, 2006; *Dutay et al.*, 2009]. The degradation rate of big and small POC has the same temperature dependance. PISCES includes parameterization of zooplankton flux feeding and (dis)aggregation, with (dis)aggregation processes allowing transfer of material between the dissolved organic carbon pool and large and small particle pools [*Gehlen et al.*, 2006]. The PISCES output is from a climatological ocean-only run at 2°, monthly resolution, with output extracted from Southern Ocean sampling stations. Processes controlling interactions between detrital pools, turbulence, and differential settling speeds decrease below the mixed layer. In the standard model version, flux feeding does not redistribute particles from large to small POC. These two models, with differing approaches to particle parameterization, allow investigation into whether the processes acting on small and large POC pools affect the predicted dynamics of slow-sinking POC fluxes and whether these processes may be driving observed variability in the SS_{POC} flux.

3. Results and Discussion

3.1. Limitations

MSCs allow a 95 L snapshot of fast-sinking, slow-sinking, and suspended POC to be sampled, which can record high variability in POC, due to the patchy nature of production and export in the upper ocean.

Originally, MSCs were designed to capture large rare particles with minimal disturbance from turbulence [*Lampitt et al.*, 1993] and often the main focus of MSC sampling is still fast-sinking particles. The carbon content of fast-sinking particles collected from MSCs has, until recently [*Belcher et al.*, 2016b], always been calculated using imaging and *Alldredge* [1998] conversion factors. However, *Bishop et al.* [2016] recently reported that *Alldredge* [1998] conversion factors underestimate the carbon content of aggregates considerably. In the future we would recommend measuring POC of the fast-sinking particles directly as in *Belcher et al.* [2016b] but as this study is a retrospective data collation, using conversion factors is unavoidable. To investigate whether conversion factors affected the results found in the Southern Ocean, we also calculate the fast-sinking POC fluxes using two conversion factors for FP [*Alldredge*, 1998; *Manno et al.*, 2015] which demonstrated differences in magnitude but minimal change in observed trends (see section 3.4).

The 2 h settling period (originally chosen to enable fast-sinking particles to reach the base of the MSC) means that not all particles that sink at a rate < 18 m d^{-1} will settle into the 8 L base. Moreover, the Giering approach assumes that the calculated SS$_{POC}$ flux is a lower limit, as the observed flux could have occurred in a shorter time than the 2 h settling period. This highlights that separating POC into three classes is an oversimplification of the true spectra of particle sinking speeds but is necessary for handling MSC samples [*Kriest and Evans*, 1999]. If the bulk of the slow-sinking material has a vastly slower sinking rate than 18 m d^{-1}, the fluxes may be an upper limit. This would also inflate our suspended POC estimates and underestimate our slow-sinking POC flux. However, the SETCOL approach may account for the slow-sinking (< 18 m d^{-1}) material as it measures the sinking time and change in mass of the initial population (slow and suspended POC).

It is worth noting that for these samples the different methods calculate very similar fluxes as they both use the dimensions of the MSC (height) and the settling time. The Giering approach calculates an in situ sinking rate for small sinking particles of ~18 m d^{-1}, whereas the SETCOL method calculates a median in situ sinking rate for small particles in the Atlantic Ocean of 22.2 (interquartile range (IQR): 14.2–29.4) m d^{-1} [*Bienfang*, 1981; *Giering et al.*, 2016]. Sinking rates of ~18 m d^{-1} and 22.2 m d^{-1} reach and exceed the upper limit we set for SS$_{POC}$ of <20 m d^{-1} but are in broad agreement with theoretical calculations by *Giering et al.* [2016] for sinking speeds of small cells based on Stoke's law. Furthermore, it is possible that the SETCOL sinking rate has a larger median than expected due to any FS$_{POC} < 100$ μm which may be included in the base and initial bulk POC measurements.

3.2. POC Concentration

Suspended POC is the largest pool in the upper Atlantic Ocean (25–650 m, median depth 100 m), with POC concentration ($\pm$ C.S.U) ranging between 8.4 ($\pm$ 0.42) and 1218.0 ($\pm$ 60.9) μg L^{-1} ($n = 144$) with a median concentration of 80.0 (interquartile range (IQR) 53.0–138.2) μg L^{-1} (Figure 2a). The SS$_{POC}$ pool is the second largest POC pool with concentration ($\pm$ C.S.U) ranging between 0.2 ($\pm$ 0.01) and 390.4 ($\pm$ 19.5) μg L^{-1} ($n = 133$), with a median of 5.5 (IQR 2.8–10.3) μg L^{-1} (Figure 2b). The FS$_{POC}$ pool ranged from 0 to 4.1 ($\pm$ 0.41) μg L^{-1} ($n = 104$) with a median of 0.07 (IQR 0.03–0.20) μg L^{-1} (Figure 2c). The POC concentrations of each pool showed large variability across sites spanning 3 orders of magnitude.

Suspended, slow, and fast POC pools occur in a 94:6:<1 ratio (based on the median of measured concentration at all sites; Table 1). Thus, most of the POC was not sinking out of the upper water column during our study (Figure 2d). The samples from the Arctic Ocean in 2012 and the South Atlantic have higher median SS$_{POC}$ and suspended POC concentration than the other regions, while the median FS$_{POC}$ concentration is consistently small in the Arctic Ocean, Subpolar North Atlantic, South Atlantic, and Southern Ocean (SO13a) and makes a greater contribution at the PAP Site and the Southern Ocean for SO13b (Figure 2d). We therefore find that sinking POC is predominantly found as SS$_{POC}$ in the Atlantic Ocean and contributes significantly to export below the MLD.

3.3. Slow-Sinking POC Flux

SS$_{POC}$ flux generally makes a greater contribution than FS$_{POC}$ flux in the Atlantic Ocean as shown by a SS$_{POC}$ flux median of 107.0 (IQR 54.2–200.8) to 99.0 (IQR 56.8–173.9) mg m^{-2} d^{-1} (Giering and SETCOL) compared to a median FS$_{POC}$ flux of 14.1 (IQR 4.6–31.4) mg m^{-2} d^{-1}. This would suggest that SS$_{POC}$ flux contributes 88.5% (IQR 70.7–97.8, $n = 94$; Giering) and 86.8% (IQR 71.7–97.3, $n = 54$; SETCOL) of the total measured POC flux in the Atlantic Ocean samples (25–650 m). These SS$_{POC}$ flux percentage contributions to
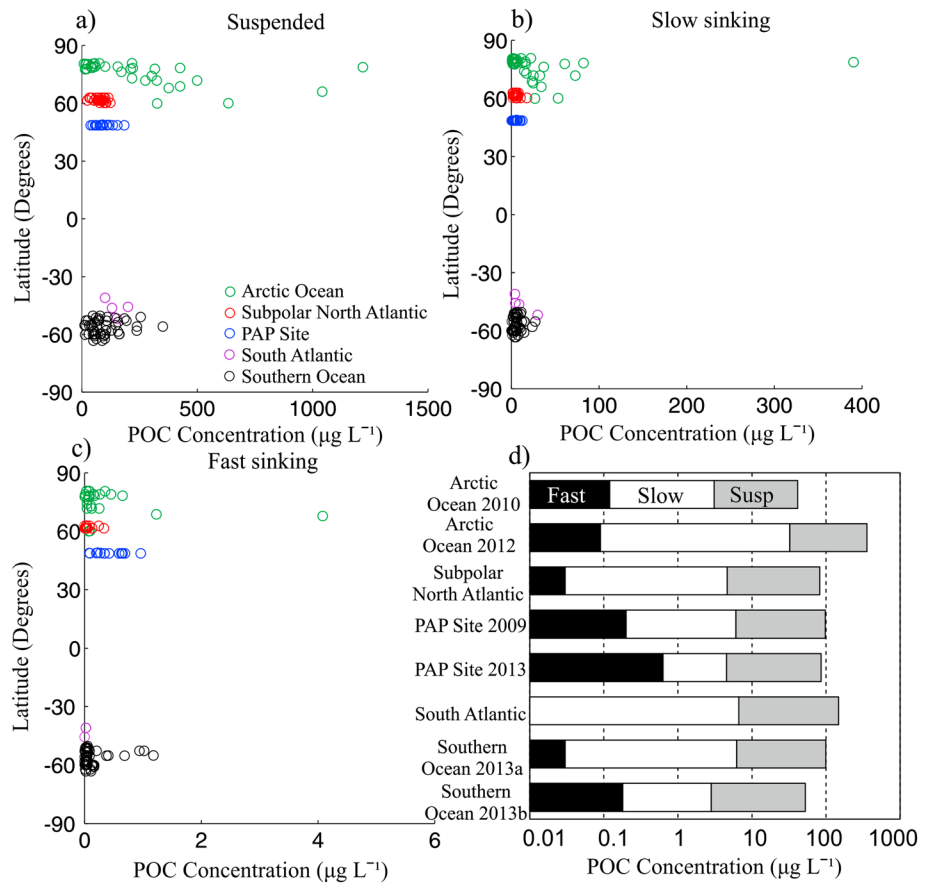
Figure 2. (a) Suspended, (b) slow-sinking, and (c) fast-sinking particulate organic carbon (POC) concentration below the mixed layer in the Atlantic Ocean plotted by latitude. Note the different *x* axis scales. (d) Median POC concentrations of the fast-sinking, slow-sinking, and suspended pools grouped by cruise (logarithmic scale).

total flux are likely to be overestimates due to the possibility of the *Alldredge* [1998] conversion factors underestimating FS$_{POC}$ flux, but the differences in magnitude highlight that SS$_{POC}$ definitely makes a substantial contribution.

Median SS$_{POC}$ fluxes observed in the Arctic Ocean contributed 57.7 (IQR 27.8–107.4) mg m^{-2} d^{-1} and 86.2% (Giering) to total flux in 2010 during a late summer chlorophyll peak (max. chlorophyll 2.1 mg m^{-3}; Figure S1). *Riley* [2012] found that diatoms contributed >50% of total carbon biomass in all samples taken during the cruise. In 2012 median SS$_{POC}$ fluxes contributed 629.0 (IQR 457–1184) mg m^{-2} d^{-1} and 98.1% (Giering) to total POC flux during a period of elevated chlorophyll concentrations associated with the spring bloom (max. of 1.8 mg m^{-3}; Table 1). In the Arctic in 2012, there was a monospecific bloom of *Phaeocystis* (*Phaeocystis Pouchetti*) near the ice edge which is suggested to explain high ^{234}Th-derived estimates of carbon export [*Le Moigne et al.*, 2015] and could potentially be responsible for the large SS$_{POC}$ fluxes (max. of 7600 mg m^{-2} d^{-1}; Data Set S1). While some marginal ice stations in the Southern Ocean in this data set also have elevated SS$_{POC}$ fluxes, none are of this magnitude, perhaps suggesting that the community structure was responsible for the major contribution of SS$_{POC}$ flux. This highlights the large contribution SS$_{POC}$ can make to export out of the MLD during major bloom events (such as those observed in 2012) and also during smaller-scale bloom events (such as those in 2010).

The PAP site in the NE Atlantic was sampled in summer 2009, after a modest summer bloom (max. chl ~1 mg m^{-3}). At this time, median SS$_{POC}$ flux was 114.2 (IQR 110–125) mg m^{-2} d^{-1} and contributed 76.5% (Giering) of total median POC flux (Table 1). In early summer 2013 the site was sampled again, in prebloom conditions (max. chl ~ 0.3 mg m^{-3}), when SS$_{POC}$ flux made up 56.8–76.1 mg m^{-2} d^{-1} (SETCOL $n = 6$, IQR

39.5–72.1 and Giering $n = 11$, and IQR 36.5–108.1, respectively) and 71.2% and 62.9% of total median POC flux. The Subpolar North Atlantic was sampled prebloom (max. chl ~0.3 mg m^{-3}) in 2012 during which the SETCOL SS$_{POC}$ flux was 96.6 (IQR 66.5–141.4, $n = 22$) mg m^{-2} d^{-1} contributing 93.5% of total flux, and the Giering SS$_{POC}$ flux was 89.6 (IQR 55.5–121.0, $n = 27$) mg m^{-2} d^{-1} contributing 97.0% of total POC flux. High prebloom SS$_{POC}$ fluxes in the Subpolar North Atlantic were attributed to the mixed layer pump with deep mixing and (dis)aggregation processes transporting particles down to 600 m (Figure S2) [*Dall'Olmo et al.*, 2016; *Giering et al.*, 2016]. Data from these sites suggest that SS$_{POC}$ flux is of smaller magnitude at the PAP Site compared to higher-latitude regions, particularly prebloom, and makes a greater contribution at lower latitudes postbloom.

In December 2013 median SS$_{POC}$ flux was 51.4 (IQR 34.0–119.2)–84.0 (IQR 30.0–160.0) mg m^{-2} d^{-1} and ~50% (Giering and SETCOL) of the total mean POC flux during the austral spring in the Southern Ocean (bloom and postbloom sampling; Table 1). A high concentration of phytoplankton cells was found in some fast-sinking samples which were associated with the bloom [*Belcher et al.*, 2016a]. SS$_{POC}$ samples taken in the Southern Ocean in January 2013, during a declining/postbloom phase, dominated total POC flux contributing 120.6 (IQR 71.5–158.8)–145.0 (IQR 82.4–249.3) mg m^{-2} d^{-1} and 91.7–94.5% to total POC flux (Giering and SETCOL, respectively). If mean POC fluxes from the Southern Ocean cruises are typical of an average year, this may suggest that SS$_{POC}$ flux becomes increasingly important from bloom to postbloom states.

The estimates of SS$_{POC}$ flux in the Atlantic Ocean presented in this study are generally at the upper limit of, or greater than, the estimated range of modeled carbon flux carried by small particles (18–78%; Sargasso Sea) [*Durkin et al.*, 2015] and the SS$_{POC}$ flux contribution from June to December (60–75%) measured in the Mediterranean Sea [*Peterson et al.*, 2005; *Alonso-González et al.*, 2010] but our bloom SS$_{POC}$ flux observations are comparable to previous studies. Small particles (1–51 μm) in the euphotic zone were sampled by *Lam et al.* [2015] in the Atlantic Ocean, and an average of 76% of POC was contained in the small-sized fraction which they deemed as nonsinking. When comparing this to the size fractionation in the MSC (0–100 μm), our percentage estimates greater than 76% seem reasonable but the two data sets have varying definitions of small/large and sinking/nonsinking particles which make direct comparisons difficult. The largest mean contributions of SS$_{POC}$ to total flux ($> 86\%$; Giering and SETCOL; Table 1) estimated for the Arctic Ocean, Subpolar North Atlantic, and the Southern Ocean exceed any previously reported observational values but support model study results by *Henson et al.* [2015] where SS$_{POC}$ contributed up to 100% of the total POC flux at high latitudes. As mentioned in section 3.1, this is likely due to fast-sinking conversion factors underestimating the total POC flux. However, as the absolute magnitude of SS$_{POC}$ fluxes is rarely published, relevant regional comparisons are not possible.

The mean SS$_{POC}$ fluxes found in the Atlantic suggest that in northern high-latitude regions SS$_{POC}$ flux is the major contributor to total flux ($> 86\%$), with the exception of lower contributions during a Southern Ocean bloom. SS$_{POC}$ flux dominates the total flux for both PAP site cruises but only contributes to 63–77% of total flux. SS$_{POC}$ flux may dominate during prebloom periods due to physical mixing to depth and (dis)aggregation of large fast-sinking particles (e.g., in the subpolar North Atlantic [*Giering et al.*, 2016]) but more generally may also be as a result of low cell concentrations inhibiting aggregate formation [*Jackson et al.*, 2005].

FS$_{POC}$ makes an increased contribution during blooms, likely due to higher concentrations of phytoplankton cells, resulting in larger/more aggregates and increasing zooplankton numbers that produce faster sinking fecal pellets (FP) [*Belcher et al.*, 2016a]. The Arctic Ocean 2012 bloom is an exception to this proposed seasonal cycle of SS$_{POC}$, potentially due to the contribution of *Phaeocystis*, which are small-celled phytoplankton [*Schoemann et al.*, 2005], to the exceptionally large POC flux. SS$_{POC}$ flux heavily dominates after the spring bloom, which we postulate is due to shifts to a smaller-sized community [*Pommier et al.*, 2009] or the fragmentation of larger particles [*Stemmann et al.*, 2004]. SS$_{POC}$ appears to make a significant contribution to flux in the upper mesopelagic in spring and summer months and to be controlled to some extent by bloom events. This is in contrast to the hypothesis *Riley et al.* [2012] proposed, in which SS$_{POC}$ is a background flux all year round and only FS$_{POC}$ flux is controlled by exceptional processes such as blooms. We speculate that SS$_{POC}$ production may be controlled predominantly by seasonality in primary production, but higher-resolution sampling throughout the year is needed to confirm this hypothesis. In future studies measuring transformations of particle flux, we recommend that a detailed record of plankton community composition
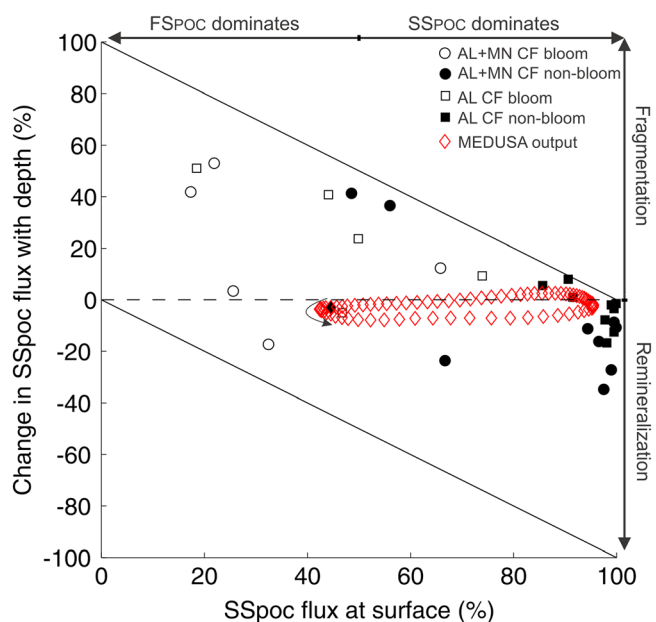
Figure 3. Percentage change in slow-sinking SETCOL POC flux with depth (SS_{POC} flux $_{(MLD + 110\ m)}$ %–SS_{POC} flux $_{(MLD + 10\ m)}$ %) versus the SETCOL SS_{POC} flux $_{(MLD + 10\ m)}$ at the surface in the Southern Ocean. The circles represent the SS_{POC} percentage fluxes when the *Alldredge* [1998] conversion factors are used for aggregates and the *Manno et al.* [2015] conversion factor is used for fecal pellets (AL + MN CF). The squares represent the SS_{POC} percentage fluxes when the *Alldredge* [1998] conversion factors are used for aggregates and fecal pellets (AL CF). This allows a comparison between the relative contributions and highlights that, while there is a change in magnitude, the trends are unchanged. The red diamonds indicate the mean annual cycle in the MEDUSA model with the black diamond representing the first time step which continues anticlockwise as shown by the arrow [*Yool et al.*, 2013]. The open symbols represent samples collected during the spring bloom in December 2013, and filled symbols represent samples collected in declining/postbloom phases in January 2013. The black diagonal lines indicate the limits of where it is mathematically possible for the SS_{POC} flux (%) to increase/decrease due to percentages being bounded by 0 and 100. Data points that plot on the zero (dashed) line show no change in the $FS:SS_{POC}$ ratio indicating both fluxes are degraded at the same rate. Data points below the dashed line indicate that SS_{POC} flux decreases in magnitude more rapidly than FS_{POC} flux. Data above the zero line indicate that SS_{POC} flux makes a greater contribution to total POC flux with depth.

and successional changes in community structure is collected to allow for a much greater analysis and discussion on the drviers of transforming particle fluxes.

3.4. Potential Controls of SS_{POC} Flux

We observed a decrease in both the magnitude of slow- and fast-sinking POC fluxes with depth (Figure S2). To further investigate changes in the sinking fluxes with depth, we compare the change in percentage contribution of SS_{POC} to total POC flux ($FS_{POC} + SS_{POC}$; Figure 3), over the measured depth range (MLD + 10 m and MLD + 110 m) in the Southern Ocean. In this way we examine the change in the relative contribution of the FS_{POC} and SS_{POC} fluxes to total flux with depth rather than the change in absolute magnitude. To attempt to account for possible underestimation of FS_{POC} fluxes due to the use of conversion factors from *Alldredge* [1998] (AL CF), we have also plotted FS_{POC} fluxes using *Alldredge* [1998] for aggregates and *Manno et al.* [2015] for fecal pellets (AL + MN CF; Figure 3). This led to some differences in magnitude at stations where FPs made a larger contribution, but overall, the trends and conclusions drawn from the plot are the same.

Samples taken during bloom conditions suggest that, at most stations, FS_{POC} dominated flux from the upper ocean with SS_{POC} making an increased relative contribution (up to 55%) to total flux deeper in the water column in some samples (Figure 3). This may be due to more rapid remineralization of FS_{POC}; however, *Cavan et al.* [2017b] found that turn over rates of SS_{POC} were at least an order of magnitude faster than FS_{POC}, which was attributed to the greater surface area to volume ratio of slow-sinking particles. A more likely process is fragmentation or disaggregation of FS_{POC}—a process which leads to in situ generation of SS_{POC} at depth. Three bloom stations did not show a sizeable increase in the contribution of SS_{POC} with depth (Figure 3), which suggests that, at these sites, there was little supply of SS_{POC} at depth via the disaggregation/fragmentation of FS_{POC}. It is possible that (dis)aggregation processes were responsible for the shifts between the fast- and slow-sinking pools of POC with depth (Figure 3); however, in the majority of samples both FS_{POC} and SS_{POC} flux decrease in absolute magnitude (Data Set S1), suggesting that remineralization rather than particle transformation was the dominant loss process at these stations.

During the decline of the bloom or in postbloom periods in the Southern Ocean, when SS_{POC} flux was >90% of total flux below the MLD, the contribution of SS_{POC} flux predominantly decreased with depth (Figure 3).

This may be due to SS_{POC} flux being remineralized at a faster rate than FS_{POC} flux during nonbloom periods, supported by the findings of *Cavan et al.* [2017b] and because there is minimal FS_{POC} to fragment into SS_{POC}. Generally, our data indicate that when FS_{POC} contributes >10% to total flux below the MLD the SS_{POC} flux often increases with depth. This supports the hypothesis that the increase in SS_{POC} flux with depth is due to the fragmentation of FS_{POC} particles.

Riley et al. [2012] suggested that SS_{POC} is a constant background POC flux persisting all year round that is remineralized in the upper ocean. In contrast, our analysis instead suggests that the contribution of SS_{POC} to total flux often increases with depth when the FS_{POC} flux below the MLD is high, as observed during the seasonal bloom, possibly due to in situ generation of SS_{POC} below the MLD. SS_{POC} has been observed in MSC samples down to 600 m [*Giering et al.*, 2016], and *Durkin et al.* [2015] found that small particles increased down to 500 m while large particles (assumed to be FS_{POC}) decreased. This supports the hypothesis that, during the bloom, there is a conversion of POC from large fast-sinking particles to small slow-sinking particles as the SS_{POC} flux contribution to total flux increases deeper in the water column.

The change in FS_{POC}:SS_{POC} ratio with depth appears to be large (up to 55%) as the FS_{POC} flux may be significantly reduced due to fragmentation/ disaggregation channelling FS_{POC} to SS_{POC}. At stations during the SO13b cruise where *Belcher et al.* [2016a] found higher attenuation of fluxes of FS_{POC} and FP, we found that SS_{POC} flux increased relatively with depth. The stations with high FS_{POC} attenuation were dominated by small copepods which are more likely to repackage POC into smaller FP, leading to retention in the upper mesopelagic [*Noji et al.*, 1991; *Belcher et al.*, 2016a]. At bloom stations, when FS_{POC} flux dominated total flux and there was no change or a decrease in SS_{POC} flux with depth, FPs contributed >80% to FS_{POC} flux at MLD + 110 m and attenuation of FS_{POC} flux was lower (Figures 3 and S3).

This may indicate an active zooplankton community undertaking diel vertical migration and active transport of POC to depth. *Belcher et al.* [2016a] suggested that at high attenuation stations, microbial respiration was insufficient to explain losses in FP flux in the upper mesopelagic, suggesting that fragmentation processes may dominate. However, at stations where the little attenuation of FS_{POC} flux with depth was observed, microbial respiration was sufficient to account for the small losses in FS_{POC} flux with depth. Therefore, reduced fragmentation processes at low attenuation stations may have minimized the transfer of POC from the FS_{POC} to the SS_{POC} pool explaining our observations of only minimal changes in the relative amount of SS_{POC} flux with depth at these stations.

Cavan et al. [2015] examined the FP flux in the Southern Ocean during the declining/postbloom phase. For stations where SS_{POC} fluxes (%) increased with depth, there was a high attenuation of FPs with depth, similar to the bloom data. Therefore, differences in the degree of fragmentation (potentially driven by differences in bloom timing and zooplankton community structure, diel vertical migration, or active transport) may explain some of the patterns we observed in the changing contribution of SS_{POC} flux with depth.

To further investigate our hypothesis of in situ production at depth, we calculated the microbial respiration rates and remineralization length scales for the slow-sinking POC fluxes for both Southern Ocean cruises using temperature adjusted respiration rates from *Cavan et al.* [2017b] (Table 2). For the SO13a cruise (postbloom) a respiration rate of 1.61 d^{-1} and a RLS of 14.42 m were estimated and for the SO13b cruise (bloom) a respiration rate of 1.34 d^{-1} and a RLS of 12.39 m were estimated. Therefore, for the 100 m between MLD + 10 m and MLD + 110 m, where 63% for SS_{POC} fluxes are remineralized every 12–14 m, < 0.1% of the original slow-sinking POC flux would remain, if there was no in situ production of slow-sinking material. Without in situ production of slow-sinking particles the fraction of flux surviving to MLD + 110 m would be further reduced if zooplankton-mediated alteration or consumption of detritus was also considered.

Microbial respiration of fast-sinking POC flux is often found to be too slow to explain observed decreases in flux [*Belcher et al.*, 2016b] which suggests that zooplankton processing may have significant interactions with fast-sinking particles. Several recent papers have concluded that zooplankton sloppy feeding [*Giering et al.*, 2014], microbial gardening [*Mayor et al.*, 2014], and zooplankton fragmentation [*Cavan et al.*, 2015; *Belcher et al.*, 2016a; *Cavan et al.*, 2017a] may lead to the in situ production of slow-sinking particles from fast-sinking particles.

Table 2. Median Values (± C.S.U.) of Parameters Used to Calculate the Temperature Adjusted Respiration Rate and the Remineralization Length Scale of Slow-Sinking POC Fluxes for Both Southern Ocean Cruises in 2013

Cruise	Median Slow-Sinking Rate (m d^{-1})	Median Temperature (°C)	Temperature Adjusted Respiration Rate (d^{-1})	Remineralization Length Scale (RLS; m)
SO2013a	23.22 (± 4.5)	2.61	1.61	14.42 (± 2.8)
SO2013b	16.60 (± 2.8)	0.66	1.34	12.39 (± 2.1)

Overall, we suggest that there is an evolution in flux character from bloom to nonbloom states, at least in the Southern Ocean, with FS$_{POC}$ dominating surface flux during blooms leading to SS$_{POC}$ flux increasing at depth, likely via fragmentation by zooplankton. SS$_{POC}$ then dominates flux throughout the upper mesopelagic during declining/postbloom conditions. This may indicate a seasonal cycle of POC flux, in terms of whether SS$_{POC}$ or FS$_{POC}$ dominates, but this hypothesis requires further investigation with samples collected during the entire seasonal cycle. The proposed mechanism of in situ production of SS$_{POC}$ below the MLD may allow for SS$_{POC}$ to be generated deeper in the mesopelagic than SS$_{POC}$ particles would usually penetrate to via direct sinking from the surface supported by respiration rates and RLS estimates. In situ SS$_{POC}$ generation in the upper mesopelagic likely results in a shallower remineralization of POC than would occur if large fast-sinking particles persisted and sank quickly through the mesopelagic zone.

3.5. Modeling POC Fluxes

To verify that fragmentation/(dis)aggregation is the dominant process controlling the increasing contribution of SS$_{POC}$ to total flux with depth, we analyzed model output from two biogeochemical models. We sampled model output over a yearly cycle which allows us to assess shifts in the relative contribution of SS$_{POC}$ to FS$_{POC}$ in response to bloom dynamics to the extent resolved by model parameterization.

We examined data from the NEMO-MEDUSA model, which does not include parameterizations of (dis)aggregation or fragmentation and no transfer of particles from the fast to the slow-sinking detrital pool [*Yool et al.*, 2013]. The model fails to reproduce MSC observations of SS$_{POC}$ flux contributing more to total flux at depth (Figure 3). During the prebloom period when SS$_{POC}$ flux is >90% and during the early bloom, both fluxes make an almost constant contribution with depth, whereas middle bloom to postbloom, SS$_{POC}$ flux contributes less to total flux with depth with smaller shifts between FS$_{POC}$ and SS$_{POC}$ pools than in our observations. This highlights that the MEDUSA model is not of sufficient complexity to capture the changes between the fast- and slow-sinking POC fluxes in the upper ocean compared to our observations of relative increases in SS$_{POC}$ flux with depth.

To explore whether models that incorporate (dis)aggregation and flux feeding capture the observed pattern in the data we analyzed PISCES model output [*Gehlen et al.*, 2006], which explicitly includes (dis)aggregation/fragmentation processes. The PISCES model allows for a much smaller contribution of SS$_{POC}$ to flux compared to the MEDUSA model, but showed similar results to MEDUSA, with no increase in small POC particles with depth which decreased relative to fast-sinking POC throughout the year (Figure 4). *Gehlen et al.* [2006] tested a variety of parameterizations of particle dynamics, including one (STD3) which doubles flux feeding by zooplankton. It may be hypothesized to cause SS$_{POC}$ flux to increase with depth due to fragmentation, but it is actually smaller in magnitude and is remineralized to a greater degree than in the standard version (STD1). In the standard model version, flux feeding does not redistribute particles from large to small POC and processes controlling the detrital pools decrease below the mixed layer. Flux feeding does, however, consume large particles, but the remineralization of small POC which sinks slowly (3 m d^{-1}) likely precludes small POC making an increased relative contribution with depth in the model.

Gehlen et al. [2006] carried out model experiments using PISCES and found that increasing flux feeding did reduce overall sinking speed and increase remineralization in the mesopelagic supporting our conclusions above. This led to an overall shallower penetration of POC in the water column and a reduced POC flux at the sediment-water interface, which was smaller than observed O$_2$ fluxes. This may be due to large particles, consumed by flux feeding, not transfering any POC to the small POC pool and instead transfering organic C to the dissolved pool. Aggregate formation was found to be a key mechanism for transferring POC at the base of the mixed layer, while flux feeding, a proxy for zooplankton activity, controlled the attenuation of fluxes in the mesopelagic.
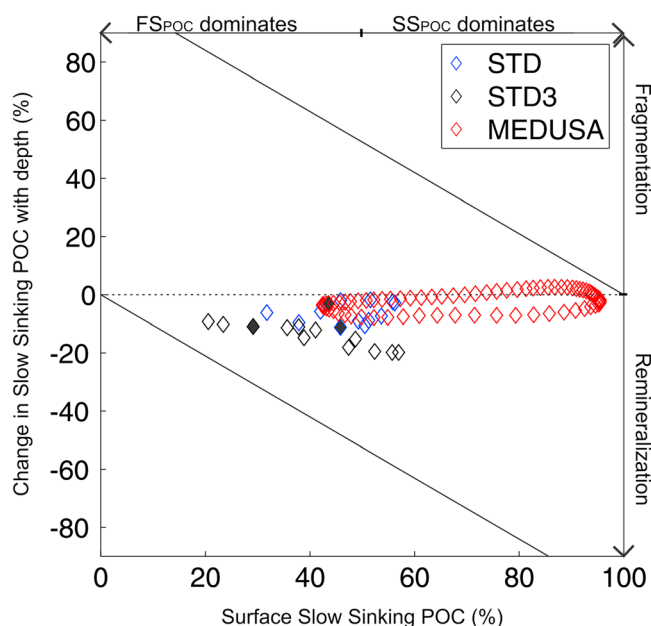
Figure 4. The change in the amount of slow-sinking POC (%) over 100 m of the upper ocean corresponding to the amount of slow-sinking POC (%) in the surface (MLD + 10 m = 45 m and MLD + 110 m = 142 m). STD is the standard PISCES model run, while the STD3 is a model run that has doubled the amount of flux feeding by zooplankton [*Gehlen et al.*, 2006]. The MEDUSA model data are the same data in Figure 3 plotted for comparison [*Yool et al.*, 2013]. The black diamonds indicate the first measurement in January of the seasonal cycle within the models continuing anticlockwise. PISCES data are monthly output, whereas MEDUSA output had a 5 day time step. The black diagonal lines indicate the limits of where it is mathematically possible for the SS_{POC} flux (%) to increase/decrease due to percentages being bounded by 0 and 100.

A more recent version of the PISCES model by *Aumont et al.* [2015] accounts for variable lability of POC. Compared to the standard version of the model [*Aumont et al.*, 2015], POC concentrations increase by up to 2 orders of magnitude in the interior ocean, providing a much improved representation when compared with observations [*Aumont et al.*, 2017]. Small particles were found to contribute ~20% to global export due to refractory POC building up in small particles, which while sinking slowly from the surface, avoid extensive remineralization during transit to the deep ocean. *Dutay et al.* [2009] also found that an increased small particle pool, with a ballast component at depth, provides a much better representation of tracers such as ^{230}Th and ^{231}Pa. When condensing knowledge from such model studies with upper ocean observations, it appears that slow-sinking particles in the upper ocean are labile [*Alonso-González et al.*, 2010] and rapidly turned over compared to fast-sinking particles [*Cavan et al.*, 2017b], with no ballast effect [*Riley et al.*, 2012], while in the deep ocean modeled slow-sinking particles have aged and so are refractory and may have a ballast component [*Dutay et al.*, 2009; *Aumont et al.*, 2017].

Our results therefore highlight the need for further particle flux observations, along with the characterization of particles throughout the water column, to clearly understand the processes modulating the fluxes of the different POC pools in the mesopelagic so that models can more robustly parameterize them. Our data suggest that, without the correct processes, increasing model complexity does not necessarily allow for better replication of observations.

4. Conclusions

We found that most POC in the Atlantic Ocean does not sink out of the upper water column. The SS_{POC} pool appears to be the largest sinking POC pool in the majority of the Atlantic Ocean. SS_{POC} dominates the total flux, except during the spring bloom in the Southern Ocean. The contribution of SS_{POC} to total flux may increase with depth when FS_{POC} flux contributes >10% to total flux in the Southern Ocean. We suggest that SS_{POC} was generated in situ below the MLD in the Southern Ocean, during the seasonal bloom, likely via fragmentation which causes high attenuation of FS_{POC} in the upper water column. As well as quantifying the significance of SS_{POC} within the upper ocean, this finding highlights the importance of identifying and determining the roles of mesopelagic processes in the transfer of POC to depth. Our model analysis suggests that the biological processes driving the transfer of particles from fast- to slow-sinking pools need to be more robustly modeled to capture the contribution of SS_{POC} to upper mesopelagic fluxes and the effect on the remineralization depth of POC. In situ generation of SS_{POC} below the mixed layer may allow slow-sinking particles to penetrate deeper than is currently parameterized in models while fast-sinking particles may have a

shallower remineralization depth than currently modeled. This may suggest that current models overestimate the importance of particle export to carbon storage as they do not accurately predict fragmentation or shifts between particle pools, which may have strong implications for modeled estimates of long-term carbon storage.

References

Alldredge, A. (1998), The carbon, nitrogen and mass content of marine snow as a function of aggregate size, *Deep Sea Res., Part I*, *45*(4–5), 529–541, doi:10.1016/S0967-0637(97)00048-4.

Alldredge, A. L., and M. W. Silver (1988), Characteristics, dynamics and significance of marine snow, *Prog. Oceanogr.*, *20*(1), 41–82, doi:10.1016/0079-6611(88)90053-5.

Alonso-González, I. J., J. Arístegui, C. Lee, A. Sanchez-Vidal, A. Calafat, J. Fabrés, P. Sangrá, P. Masqué, A. Hernández-Guerra, and V. Benítez-Barrios (2010), Role of slowly settling particles in the ocean carbon cycle, *Geophys. Res. Lett.*, *37*, LI3608, doi:10.1029/2010GL043827.

Armstrong, R. A., C. Lee, J. I. Hedges, S. Honjo, and S. G. Wakeham (2002), A new, mechanistic model for organic carbon fluxes in the ocean: Based on the quantitative association of POC with ballast minerals, *Deep Sea Res., Part II*, *49*, 219–236.

Aumont, O., and L. Bopp (2006), Globalizing results from ocean *in situ* iron fertilisation studies, *Global Biogeochem. Cycles*, *20*, GB2017, doi:10.1029/2005GB002591.

Aumont, O., C. Ethé, A. Tagliabue, L. Bopp, and M. Gehlen (2015), PISCES-v2: An ocean biogeochemical model for carbon and ecosystem studies, *Geosci. Model Dev.*, *8*, 2465–2513, doi:10.5194/gmd-8-2465-2015.

Aumont, O., M. van Hulten, M. Roy-Barman, J.-C. Dutay, C. Éthé, and M. Gehlen (2017), Variable reactivity of particulate organic matter in a global ocean biogeochemical model, *Biogeosciences*, *14*, 2321–2341, doi:10.5194/bg-2016-374.

Becquevort, S., and W. O. Smith Jr. (2001), Aggregation, sedimentation and biodegradability of phytoplankton-derived material during spring in the Ross Sea, Antarctica, *Deep Sea Res., Part II*, *48*, 4155–4178.

Belcher, A., M. Iversen, C. Manno, S. A. Henson, G. A. Tarling, and R. Sanders (2016a), The role of particle associated microbes in remineralization of fecal pellets in the upper mesopelagic of the Scotia Sea, Antarctica, *Limnol. Oceanogr.*, *61*, 1049–1064, doi:10.1002/lno.10269.

Belcher, A., M. Iversen, S. Giering, V. Riou, S. A. Henson, L. Berline, L. Guilloux, and R. Sanders (2016b), Depth-resolved particle-associated microbial respiration in the northeast Atlantic, *Biogeosciences*, *13*, 4943–4943, doi:10.5194/bg-13-4927-2016.

Bienfang, P. K. (1981), SETCOL—A technologically simple and reliable method for measuring phytoplankton sinking rates, *Can. J. Fish. Aquat. Sci.*, *38*, 1289–1294.

Billett, D. S. M., R. S. Lampitt, A. L. Rice, and R. F. C. Mantoura (1983), Seasonal sedimentation of phytoplankton to the deep-sea benthos, *Nature*, *302*, 520–522.

Bishop, J. K. B., M. B. Fong, and T. J. Wood (2016), Robotic observations of high wintertime carbon export in California coastal waters, *Biogeosciences*, *13*, 3109–3129, doi:10.5194/bg-13-3109-2016.

Bopp, L., O. Aumont, P. Cadule, S. Alvain, and M. Gehlen (2005), Response of diatom distribution to global warming and potential implications: A global model study, *Geophys. Res. Lett.*, *32*, L19606, doi:10.1029/2005GL023653.

Boyd, P. W., and T. W. Trull (2007), Understanding the export of biogenic particles in oceanic waters: Is there consensus?, *Prog. Oceanogr.*, *72*, 276–312.

Buesseler, K. O., et al. (2007), An assessment of the use of sediment traps for estimating upper ocean particle fluxes, *J. Mar. Res.*, *65*, 345–416.

Burd, A. B., and G. A. Jackson (2009), Particle aggregation, *Annu. Rev. Mar. Sci.*, *1*, 65–90, doi:10.1146/annurev.marine.010908.163904.

Cavan, E. L., F. A. C. Le Moigne, A. J. Poulton, G. A. Tarling, P. Ward, C. J. Daniels, G. M. Fragoso, and R. J. Sanders (2015), Attenuation of particulate organic carbon flux in the Scotia Sea, Southern Ocean, is controlled by zooplankton fecal pellets, *Geophys. Res. Lett.*, *42*, 821–830, doi:10.1002/2014GL062744.

Cavan, E. L., S. A. Henson, A. Belcher, and R. Sanders (2017a), Role of zooplankton in determining the efficiency of the biological carbon pump, *Biogeosciences*, *14*, 177–186, doi:10.5194/bg-14-177-2017.

Cavan, E. L., M. Trimmer, F. Shelley, and R. Sanders (2017b), Remineralization of particulate organic carbon in an ocean oxygen minimum zone, *Nat. Commun.*, *8*, doi:10.1038/ncomms14847.

Close, H. G., S. R. Shah, A. E. Ingalls, A. F. Diefendorf, E. L. Brodie, R. L. Hansman, K. H. Freeman, L. I. Aluwihare, and A. Pearson (2013), Export of submicron particulate organic matter to mesopelagic depth in an oligotrophic gyre, *Proc. Natl. Acad. Sci.*, *110*(31), 12,565–12,570, doi:10.1073/pnas.1217514110.

Dall'Olmo, G., and K. A. Mork (2014), Carbon export by small particles in the Norwegian Sea, *Geophys. Res. Lett.*, *41*, 2921–2927, doi:10.1002/2014GL059244.

Dall'Olmo, G., J. Dingle, L. Polimene, R. J. W. Brewin, and H. Claustre (2016), Substantial energy input to the mesopelagic ecosystem from the seasonal mixed-layer pump, *Nat. Geosci.*, doi:10.1038/NGEO2818.

Dilling, L., and A. L. Alldredge (2000), Fragmentation of marine snow by swimming macrozooplankton: A new process impacting carbon cycling in the sea, *Deep Sea Res., Part I*, *47*(7), 1227–1245, doi:10.1016/S0967-0637(99)00105-3.

Durkin, C. A., M. L. Estapa, and K. O. Buesseler (2015), Observations of carbon export by small sinking particles in the upper mesopelagic, *Mar. Chem.*, *175*, 72–81, doi:10.1016/j.marchem.2015.02.011.

Dutay, J. C., F. Lacan, M. Roy-Barman, and L. Bopp (2009), Influence of particle size and type on 231Pa and 230Th simulation with a global coupled biogeochemical-ocean general circulation model: A first approach, *Geochem. Geophys. Geosyst.*, *10*, Q01011, doi:10.1029/2008GC002291.

Gardner, W. D., S. P. Chung, M. J. Richardson, and I. D. Walsh (1995), The oceanic mixed-layer pump, *Deep Sea Res., Part II*, *42*(2), 757–775.

Gehlen, M., L. Bopp, N. Emprin, O. Aumount, C. Heinze, and O. Ragueneau (2006), Reconciling surface ocean productivity, export fluxes and sediment composition in a global biogeochemical ocean model, *Biogeosciences*, *3*, 521–537.

Giering, S. L., et al. (2014), Reconciliation of the carbon budget in the ocean's twilight zone, *Nature*, *307*, 480–483, doi:10.1038/nature13123.

Giering, S. L. C., R. Sanders, A. P. Martin, C. Lindemann, K. O. Möller, C. J. Daniels, D. J. Mayor, and M. A. S. John (2016), High export via small particles before the onset of the North Atlantic spring bloom, *J. Geophys. Res. Oceans*, *121*, 6929–6945, doi:10.1002/2016JC012048.

Goutx, M., S. G. Wakeham, C. Lee, M. Duflos, C. Guigue, Z. Liu, B. Moriceau, R. Sempéré, M. Tedetti, and J. Xue (2007), Composition and degradation of marine particles with different settling velocities in the northwestern Mediterranean Sea, Limnol, *Oceanography*, *52*(4), 1645–1664.

Henson, S. A., A. Yool, and R. Sanders (2015), Variability in efficiency of particulate organic carbon export: A model study, *Global Biogeochem. Cycles*, *29*, 33–45, doi:10.1002/2014GB004965.

Iversen, M. H., and H. Ploug (2013), Temperature effects on carbon-specific respiration rate and sinking velocity of diatom aggregates—Potential implications for deep ocean export processes, *Biogeosciences*, *10*, 4073–4085.

Iversen, M. H., and L. K. Poulsen (2007), Coprorhexy, coprophagy, and coprochaly in the copepods *Calanus helgolandicus*, *Pseudocalanus elongatus*, and *Oithona similis*, *Mar. Ecol. Prog. Ser.*, *350*, 79–89, doi:10.3354/meps07095.

Jackson, G. A., A. M. Waite, and P. W. Boyd (2005), Role of algal aggregation in vertical carbon export during SOIREE and in other low biomass environments, *Geophys. Res. Lett.*, *32*, L13607, doi:10.1029/2005GL023180.

Jumars, P., D. Penry, and J. Baross (1989), Closing the microbial loop: Dissolved carbon pathway to heterotrophic bacteria from incomplete ingestion, digestion and absorption in animals, *Deep Sea Res., Part A*, *36*, 483–495.

Kriest, I., and G. T. Evans (1999), Representing phytoplankton aggregates in biogeochemical models, *Deep Sea Res., Part I*, *46*(11), 1841–1859.

Kwon, E. Y., F. Primeau, and J. L. Sarmiento (2009), The impact of remineralization depth on the air-sea carbon balance, *Nat. Geosci.*, *2*, 630–635, doi:10.1038/NGEO612.

Lam, P. J., D. C. Ohnemus, and M. E. Auro (2015), Size-fractionated major particle composition and concentrations from the US GEOTRACES North Atlantic Zonal Transect, *Deep Sea Res., Part II*, *116*, 303–320, doi:10.1016/j.dsr2.2014.11.020.

Lampitt, R. S., T. Noji, and B. von Bodungen (1990), What happens to zooplankton faecel pellets? Implications for material flux, *Mar. Biol.*, *104*(1), 15–23, doi:10.1007/BF01313152.

Lampitt, R. S., K. F. Wishner, C. M. Turley, and M. V. Angel (1993), Marine snow studies in the Northeast Atlantic Ocean: Distribution, composition and role as a food source for migrating plankton, *Mar. Biol.*, *116*, 689–702, doi:10.1007/BF00355486.

Le Moigne, F. A. C., et al. (2015), Carbon export efficiency and phytoplankton community composition in the Atlantic sector of the Arctic Ocean, *J. Geophys. Res. Oceans*, *120*, 3896–3912, doi:10.1002/2015JC010700.

Lee, C., S. G. Wakeham, and J. I. Hedges (2000), Composition and flux of particulate amino acids and chloropigments in equatorial Pacific seawater and sediments, *Deep Sea Res., Part I*, *47*(8), 1535–1568, doi:10.1016/S0967-0637(99)00116-8.

Manno, C., G. Stowasser, P. Enderlein, S. Fielding, and G. A. Tarling (2015), The contribution of zooplankton faecal pellets to deep-ocean transport in the Scotia Sea (Southern Ocean), *Biogeosciences*, *12*, 1955–1965.

Mayor, D. J., R. Sanders, S. L. C. Giering, and T. R. Anderson (2014), Microbial gardening in the ocean's twilight zone: Detritivorous metazoans benefit from fragmenting, rather than ingesting, sinking detritus, *BioEssays*, *36*(12), 1132–1137, doi:10.1002/bies.201400100.

Noji, T. T., K. W. Estep, F. Macintyre, and F. Norrbin (1991), Image analysis of faecal material grazed upon by three species of copepods: Evidence for coprorhexy, coprophagy and coprochaly, *J. Mar. Biol. Assoc.*, *71*, 465–480.

Peterson, M. L., S. G. Wakeham, C. Lee, M. A. Askea, and J. C. Miquel (2005), Novel techniques for collection of sinking particles in the ocean and determining their settling rates, *Limnol. Oceanogr. Methods*, *3*, 520–532, doi:10.4319/lom.2005.3.520.

Ploug, H., and B. B. Jorgensen (1999), A net-jet flow system for mass transfer and microsensor studies of sinking aggregates, *Mar. Ecol. Prog. Ser.*, *176*, 279–290, doi:10.3354/meps176279.

Ploug, H., A. Terbrüggen, A. Kaufmann, D. Wolf-Gladrow, and U. Passow (2010), A novel method to measure particle sinking velocity in vitro, and its comparison to three other in vitro methods, *Limnol. Oceanogr.*, *8*, 386–393, doi:10.4319/lom.2010.8.386.

Pommier, J., M. Gosselin, and C. Michel (2009), Size-fractionated phytoplankton production and biomass during the decline of the northwest Atlantic spring bloom, *J. Plankton Res.*, *31*(4), 429–446.

Riley, J. S. (2012), Quantification and characterisation of particle export into the mesopelagic, PhD thesis Univ. of Southampton.

Riley, J. S., R. Sanders, C. Marsay, F. A. C. Le Moigne, E. P. Achterberg, and A. J. Poulton (2012), The relative contribution of fast and slow sinking particles to ocean carbon export, *Global Biogeochem. Cycles*, *26*, GB1026, doi:10.1029/2011GB004085.

Schoemann, V., S. Becquevort, J. Stefels, V. Rousseau, and C. Lancelot (2005), Phaeocystis blooms in the global ocean and their controlling mechanisms: A review, *J. Sea Res.*, *53*, 43–66, doi:10.1016/j.seares.2004.01.008.

Smith, H. E. K. (2014), The contribution of mineralising phytoplankton to the biological carbon pump in high latitudes, PhD thesis Univ. of Southampton.

Stemmann, L., G. A. Jackson, and D. Ianson (2004), A vertical model of particle size distributions and fluxes in the midwater column that includes biological and physical processes—Part I: Model formulation, *Deep Sea Res., Part I*, *51*, 885–908, doi:10.1016/j.dsr.2004.03.001.

Stewart, G. M., S. B. Moran, and M. W. Lomas (2010), Seasonal POC fluxes at BATS estimated from [210]Po deficits, *Deep Sea Res., Part I*, *57*, 113–124, doi:10.1016/j.dsr.2009.09.007.

Suess, E. (1980), Particulate organic carbon flux in the oceans—Surface productivity and oxygen utilisation, *Nature*, *288*, 260–263.

Villa-Alfageme, M., F. de Soto, A. C. Le Moigne, S. L. C. Giering, R. Sanders, and R. Garcia-Tenorio (2014), Observations and modelling of slow-sinking particles in the twilight zone, *Global Biogeochem. Cycles*, *28*, 1327–1342, doi:10.1002/2014GB004981.

Villa-Alfageme, M., F. C. de Soto, E. Ceballos, S. L. C. Giering, F. A. C. Le Moigne, S. Henson, J. L. Mas, and R. J. Sanders (2016), Geographical, seasonal and depth variation in sinking particle speeds in the North Atlantic, *Geophys. Res. Lett.*, *43*, 8609–8616, doi:10.1002/2016GL069233.

Volk, T. and M. I. Hoffert (1985), Ocean carbon pumps: Analysis of relative strengths and efficiencies in ocean-driven atmospheric CO_2 changes, in *The Carbon Cycle and Atmospheric CO: Natural Variations Archean to Present*, pp. 99–110, edited by E. T. Sundquist and W. S. Broecker, AGU, Washington, D. C., doi:10.1029/GM032p0099.

Yool, A., E. E. Popova, and T. R. Anderson (2013), MEDUSA-2.0: An intermediate complexity biogeochemical model of the marine carbon cycle for climate change and ocean acidification studies, *Geosci. Model Dev.*, *6*, 1767–1811, doi:10.5194/gmd-6-1767-2013.

Yool, A., E. E. Popova, and A. C. Coward (2015), Future change in ocean productivity: Is the Arctic the new Atlantic?, *J. Geophys. Res. Oceans*, *120*, 7771–7790, doi:10.1002/2015JC011167.

Yvon-Durocher, G., et al. (2012), Reconciling the temperature dependence of respiration across timescales and ecosystem types, *Nature*, *487*, 472–476, doi:10.1038/nature11205.